Journal of Catalysis **204,** 192–199 (2001)
doi:10.1006/jcat.2001.3357, available online at http://www.idealibrary.com on IDEAL®

Influence of the Dispersion of Metallic Particles on the Reaction of Triphenylarsine with Alumina-Supported Nickel

V. Maurice,* Yu. A. Ryndin,* G. Bergeret,† L. Savary,‡ J. P. Candy,*,[1] and J. M. Basset,*

*Laboratoire de Chimie Organo-Métallique de Surface-CPE, 43 bd. du 11 Novembre 1918, 69616 Villeurbanne, France; †Institut de Recherches sur la Catalyse, CNRS, 2 Av. Albert Einstein, 69626 Villeurbanne Cedex, France; and ‡Institut Français du Pétrole, 1–4 Av. de Bois-Préau, 92506 Rueil Malmaison, France

Received May 15, 2001; revised July 19, 2001; accepted July 20, 2001

The hydrogenolysis of triphenylarsine with alumina-supported nickel catalysts with various particle sizes was studied at temperatures ranging from 303 to 443 K under 12 bar of hydrogen. The reaction initially takes place selectively on the surface of the nickel particles and leads to the successive hydrogenolysis of –As–Ph bonds with benzene and cyclohexane formation. At 303 K, the reaction stops when the Ni particles are completely covered with grafted–As–Ph fragments. The quantity of fixed arsenic increases with the dispersion of the metal particles. It is proposed that more As–Ph fragments (per metallic atom) are grafted onto edge atoms than onto face atoms of the Ni particles. When the reaction is performed at higher temperature, the As atoms migrate inside the nickel particles easily and form an intermetallic compound. At 373 K, the Ni_5As_2 phase, very poorly crystallized, is obtained. At 443 K, the reaction leads to a well-crystallized phase NiAs. The dispersion of the catalyst has no influence on the nature of the formed intermetallic species. However, the formation rate of these species increases with the dispersion of the catalysts. © 2001 Academic Press

Key Words: **nickel catalyst; catalyst poisoning (arsenic); particle size effect.**

1. INTRODUCTION

The presence of arsine compounds in crude oil or in raw condensates can cause corrosion of equipment, reduction of catalyst life, and environmental pollution (1–4). Arsenic present as organometallic compounds in nonolefinic liquid hydrocarbons can be completely removed by feedstock treatment on nickel-based solids under hydrogen at 433–473 K (5–8).

It was demonstrated that triphenylarsine, used as a model compound, reacts readily under hydrogen at 400 K on the metallic surface of alumina-supported nickel, with benzene evolution and formation of As atoms. As previously observed with AsH_3, these As atoms penetrate into the metallic particle to form, in a first step, intermetallic phases Ni_xAs_y and then the well-characterized NiAs nickeline alloy (2, 9, 10). The interaction between $AsPh_3$ and Ni is typically a reaction of Surface Organo-Metallic Chemistry on Metals (SOMC/M) (11), which deal with the study and application of reaction between organometallic compounds and metallic surfaces.

The aim of this work is to study the mechanism of the triphenylarsine ($AsPh_3$) interaction with metallic nickel catalysts at different temperatures and for different nickel particle sizes. The behavior of the reaction with $AsPh_3$ is compared to that observed with $SnBu_4$ used as a probe molecule.

2. EXPERIMENTAL

2.1. Catalysts and Reactants

Alumina-supported nickel was prepared by the incipient wetness procedure. The alumina surface area was measured by N_2 adsorption and the metal loading was measured by elemental analysis.

The amount of adsorbed hydrogen at 298 K on the samples was measured using a volumetric apparatus already described (12). The sample was reduced in flowing hydrogen at increasing temperature (1.7 K/min from 300 to 673 K and 4 h at 673 K). It was then evacuated at 673 K for 4 h and cooled down to room temperature under vacuum, prior to adsorption measurements. The dispersion of the samples (number of surface nickel atoms per total nickel atoms, $D = Ni_s/Ni_t$) was deduced from the amount of hydrogen chemisorbed at 298 K under 15 kPa, using the accepted stoichiometry of 1 chemisorbed hydrogen atom per surface nickel atom ($H/Ni_s = 1$) (13, 14).

The magnetization (σ) of the samples was measured in an electromagnetic field (H) varying from 0 to 21 kOe at room temperature using the extraction method (15). The samples were taken directly from the autoclave, in *n*-heptane solution, under flowing argon and placed in the magnetization sample holder, in *n*-heptane, without contact with air. After magnetization measurement, the samples were dried and weighted. The magnetization at saturation expressed in

[1] To whom correspondence should be addressed.

0021-9517/01 $35.00

Bohr magneton per Ni (β/Ni) is obtained by extrapolation of the $\sigma = f(1/H)$ curve for $1/H \rightarrow 0$ (16). The average metallic particle size can be estimated from the $\sigma = f(H)$ curve (17). The dispersion of the samples ($D = Ni_s/Ni_t$) was deduced from the average particle size, assuming a cubooctahedral shape for the metallic particles (18).

X-ray diffraction patterns were obtained with a Bruker D5005 Theta-Theta diffractometer equipped with a diffracted-beam graphite monochromator using Cu$K\alpha$ radiation (1.54184 Å). The data were collected by continuous scanning between 15° and 73° (2θ) with a counting time of 8 s/0.02°. The recorded patterns were referred to the powder diffraction file PDF-2 Database (International Centre for Diffraction Data) for the identification of phases, using the software package DiffracPlus (Socabim-Bruker).

Tetrabutyltin ($SnBu_4$) and triphenylarsine ($AsPh_3$) were purchased from Aldrich.

The *n*-heptane used as solvent was freshly distilled and was kept in a glass flask under argon.

2.2. Triphenylarsine and Tetrabutyltin Interaction with Supported Nickel

The reactions between $AsPh_3$ and $SnBu_4$ with Ni catalysts were carried out in a magnetic drive stirred (100 mL) autoclave in 50 mL of *n*-heptane at a temperature varying between 303 and 443 K for $AsPh_3$ and at a temperature of 303 K for $SnBu_4$ under hydrogen pressure of 12 bar. Before the reaction, the desired amount of catalyst was reduced in flowing hydrogen at increasing temperature (1.7 K/min from 300 to 673 K) and 12 h at 673 K. After cooling down at room temperature under hydrogen, the reduced catalyst was impregnated by 50 mL of *n*-heptane. This suspension of catalyst was placed into the autoclave under argon and then the reactor was purged by H_2. The temperature and the pressure of the autoclave were established at the desired values and a known amount of $AsPh_3$ in solution (80 mg/50 mL) in *n*-heptane or a known amount of $SnBu_4$ in solution (90.7 mg/50 mL) in *n*-heptane was introduced into the autoclave by a syringe. The amount of $AsPh_3$ or $SnBu_4$, benzene, and cyclohexane was measured by gas chromatography (respectively HT 5 nonpolar column, 12 m × 0.22 mm × 0.5 μm, and KCl/Al_2O_3 column, 60 m × 0.32 mm × 0.5μm), of the reaction mixture, taken at regular intervals of time.

2.3. Influence of Stirring Rate and Pore Size

It was checked that the initial rate of the reaction did not depend on the stirring rate and was proportional for a given catalyst to the amount of catalyst introduced. In all the experiments, the stirring rate (SR) was 660 rpm.

It was checked that the initial rate of the reaction measured with crushed and not crushed catalysts under the same operating conditions ($P_{H_2} = 12$ bar, $T = 443$ K, SR = 660 rpm) are identical.

TABLE 1

Characteristics of the Ni/Al_2O_3 Catalysts

	NiD10	NiD18	NiD28
Ni loading (wt%)	18	25	8
Al_2O_3 specific area (m^2/g)	169	360	139
Pore size (nm)	>10	5–10	>10
Dispersion from chemisorption (%)	10.7	19.1	27.5
Dispersion from magnetism (%)	9.5	16.5	28.7
Average value for dispersion	10	18	28

3. RESULTS

3.1. Catalyst Characterization

Three alumina-supported nickel samples were prepared with nickel loading ranging from 8 to 25%.

The surface area and the pore size of the support, the metal loading, the dispersion of the samples (number of surface nickel atoms per total nickel atoms, Ni_s/Ni_t), deduced from hydrogen chemisorption and from magnetization curves, are reported in Table 1.

3.2. Triphenylarsine Interaction with Supported Nickel

3.2.1. $T = 303$ K. As seen in Fig. 1, the $AsPh_3$ interaction with Ni/Al_2O_3 at 303 K occurs selectively on the metallic surface since there is no reaction with alumina. The reaction proceeds with benzene and cyclohexane evolution. Interestingly, if cyclohexane appears immediately at the

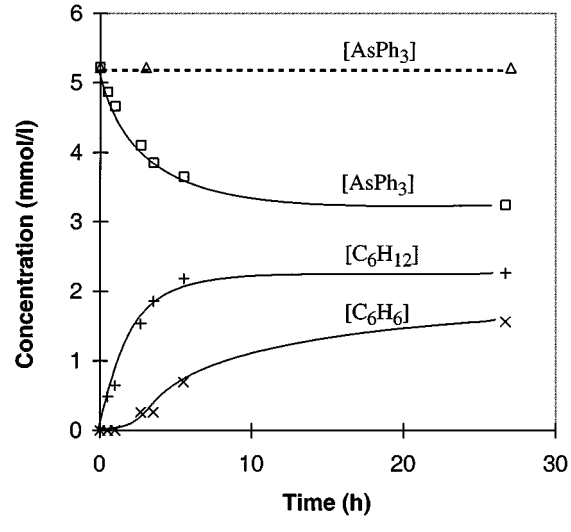

FIG. 1. Kinetics of the $AsPh_3$ reaction at 303 K under 12 bar of H_2 in 50 mL of *n*-heptane (5.22 mmol/L of $AsPh_3$), with 1 g of alumina support (dotted line) and 0.345 g of Ni/Al_2O_3, NiD28 (plain lines).

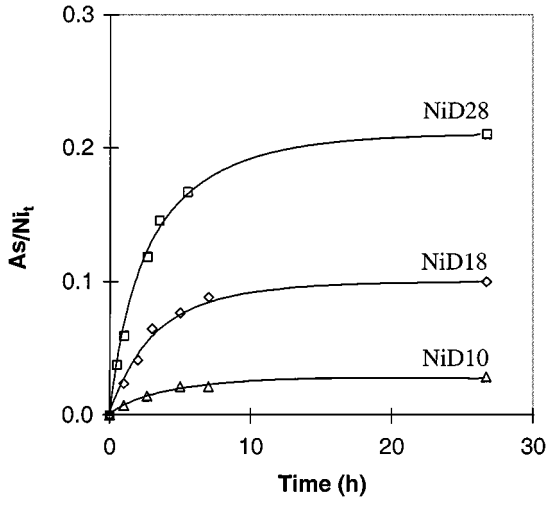

FIG. 2. Kinetics of the $AsPh_3$ reaction at 303 K under 12 bar of H_2 in 50 mL of *n*-heptane (5.22 mmol/L of $AsPh_3$), with NiD28, NiD18, and NiD10 Ni/Al_2O_3 catalysts ($AsPh_3/Ni_t = 0.6$).

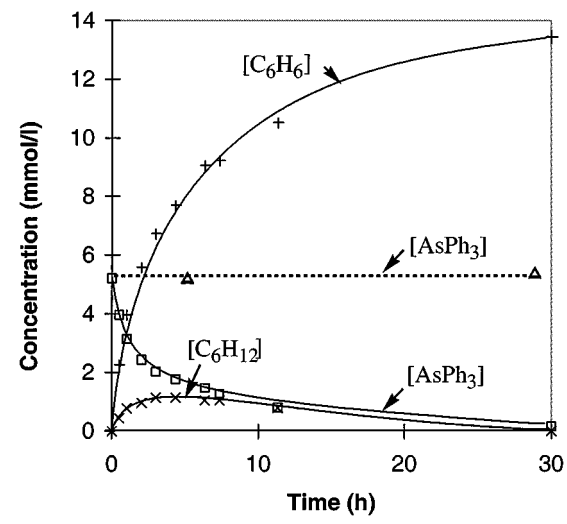

FIG. 3. Kinetics of the $AsPh_3$ reaction at 373 K under 12 bar of H_2 in 50 mL of *n*-heptane (5.22 mmol/L of $AsPh_3$), with 1 g of alumina support (dotted line) and 0.349 g of Ni/Al_2O_3, NiD28 (plain lines).

beginning of the reaction, benzene is observed only after 3 h. After about 20 h, the concentration of $AsPh_3$, benzene, and cyclohexane have reached a plateau; there is no more reaction of $AsPh_3$ with Ni.

From the data of Fig. 1, it is possible to determine the amount of $AsPh_3$ decomposed per Ni_t atom as a function of time of the reaction (Fig. 2). Increasing the dispersion of the metallic particle on the Ni catalyst (increasing the ratio Ni_s/Ni_t) clearly increases the amount of $AsPh_3$ decomposed per Ni_t atom (Fig. 2). The amount of arsenic (As atoms or $AsPh_x$ fragments) fixed on the samples per Ni_t atom (As_f/Ni_t ratio) or per Ni surface atoms (As_f/Ni_s ratio) after 24 h of reaction is reported in Table 2. The number of As species fixed on the samples is never greater than the amount of surface nickel atoms, even if the As_f/Ni_s increases with the dispersion. After 24 h of reaction, the amount of C_6 (benzene + cyclohexane) evolved per As fixed (C_6/As_f) is close to 2 for the three samples. Therefore, about one phenyl group is still present in the grafted As species (Ph/As_f).

3.2.2. $T = 373$ K. At 373 K, $AsPh_3$ does not react with Al_2O_3; there is no evolution of the $AsPh_3$ concentration and no formation of benzene or cyclohexane (Fig. 3).

With Ni/Al_2O_3, $AsPh_3$ reacts quickly with the formation of cyclohexane and benzene (Fig. 3). At this temperature, benzene is the major product. After 30 h of reaction, a *pseudo*-plateau is observed.

Increasing the dispersion of the metallic particle on the Ni catalyst (increasing the Ni_s/Ni_t ratio) increases the rate of the reaction (Fig. 4), but after 30 h, the amount of $AsPh_3$

TABLE 2

Triphenylarsine Interaction with Supported Nickel Catalysts at 303 K under 12 bar of H_2 in 50 mL of $AsPh_3$ Solution in *n*-Heptane (5.22 mmol/L)

Catalyst	NiD10	NiD18	NiD28
Ni_s/Ni_t	0.10	0.18	0.28
As_f/Ni_t	0.020	0.10	0.20
As_f/Ni_s	0.20	0.58	0.71
C_6/As_f	1.9	1.8	1.9
$x = Ph/As_f$	1.1	1.2	1.1

Note. Amount of triphenylarsine introduced per total nickel atoms ($AsPh_3/Ni_t$) = 0.6. Reaction time: 24 h; quantity of triphenylarsine fixed (As_f), per surface nickel atoms (As_f/Ni_s) or per total nickel atoms (As_f/Ni_t); quantity of C_6 (benzene + cyclohexane) evolved (C_6) per grafted $AsPh_x$ species (C_6/As_f).

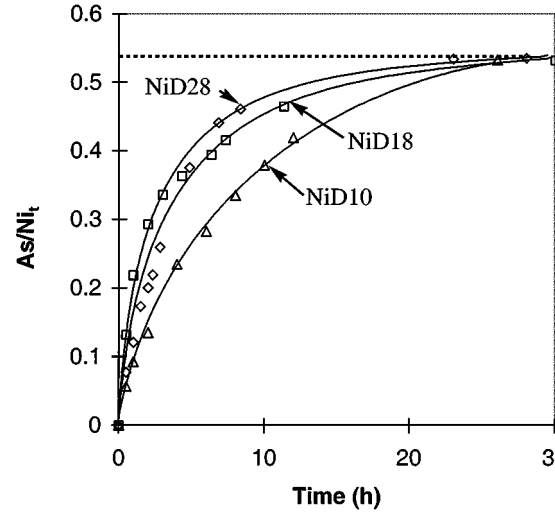

FIG. 4. Kinetics of the $AsPh_3$ reaction at 373 K under 12 bar of H_2 in 50 mL of *n*-heptane (5.22 mmol/L of $AsPh_3$), with NiD28, NiD18, and NiD10 Ni/Al_2O_3 catalysts ($AsPh_3/Ni_t = 0.6$).

TABLE 3

Triphenylarsine Interaction with Supported Nickel Catalysts at 373 K under 12 bar of H_2 in 50 mL of $AsPh_3$ Solution in *n*-Heptane (5.22 mmol/L)

Catalyst	NiD10	NiD18	NiD28
Ni_s/Ni_t	0.10	0.18	0.28
As_f/Ni_t	0.52	0.53	0.53
As_f/Ni_s	4.3	2.8	1.9
C_6/As_f	2.4	2.6	2.7
Ph/As_f	0.6	0.4	0.3

Note. Amount of triphenylarsine introduced per total nickel atoms ($AsPh_3/Ni_t$) = 0.6. Reaction time: 24 h; quantity of triphenylarsine fixed (As_f), per surface nickel atoms (As_f/Ni_s) or per total nickel atoms (As_f/Ni_t); quantity of C_6 (benzene + cyclohexane) evolved (C_6) per grafted $AsPh_x$ species (C_6/As_f).

decomposed per total Ni is approximately the same for the three samples and consequently the As_f/Ni_s ratio decreases with the dispersion, which was not the case when the reaction is performed at 303 K.

As shown in Table 3, the saturation value for $AsPh_3$ decomposition on Ni/Al_2O_3 catalysts at 373 K is close to 0.53 As/Ni_t. The amount of C_6 (benzene + cyclohexane) evolved per As fixed (C_6/As_f) is close to 2.6 for the three samples. Therefore, less than one phenyl group (Ph) is still present in the grafted As species (As_f).

3.2.3. T = 443 K. At 443 K, $AsPh_3$ reacts quickly with Ni/Al_2O_3 with the formation of cyclohexane and benzene (Fig. 5). At this temperature, benzene and cyclohexane appear simultaneously and benzene is the major product. After about 30 h of reaction, the consumption of $AsPh_3$ and the formation of benzene or cyclohexane is stopped.

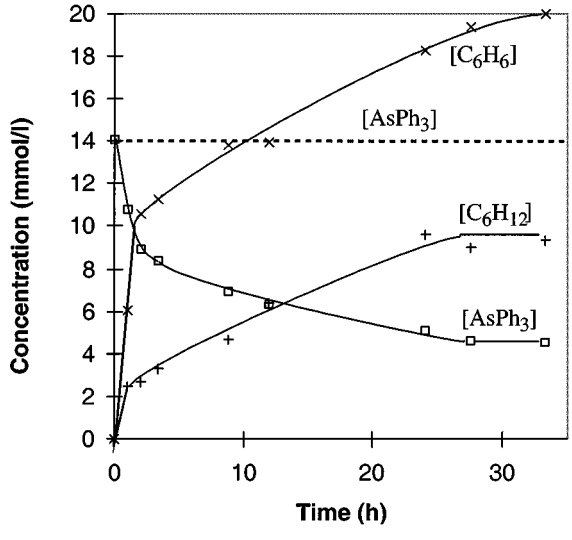

FIG. 5. Kinetics of the $AsPh_3$ reaction at 443 K under 12 bar of H_2 in 50 mL of *n*-heptane (14.1 mmol/L of $AsPh_3$), with 1 g of alumina support (dotted line) and 0.340 g of Ni/Al_2O_3, NiD28 (plain lines).

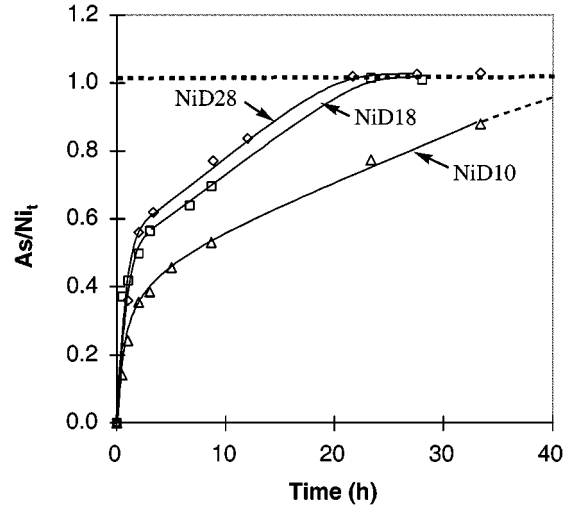

FIG. 6. Kinetics of the $AsPh_3$ reaction at 443 K under 12 bar of H_2 in 50 mL of *n*-heptane (14.1 mmol/L of $AsPh_3$), with NiD28, NiD18, and NiD10 Ni/Al_2O_3 catalysts ($AsPh_3/Ni_t$ = 1.5).

The kinetics of the reaction can be divided into two parts. The reaction is very fast from the beginning to about half of the total consumption of $AsPh_3$; then, the reaction proceeds slowly and stops after about 30 h.

Increasing the dispersion of the metallic particle on the Ni catalyst (increasing the ratio Ni_s/Ni_t) increases the rate of the two parts of the reaction (Fig. 6), but the breaking point between the fast and the slow processes is always observed in the same region.

As indicated in Table 4, the saturation value for $AsPh_3$ decomposition on the three Ni/Al_2O_3 catalysts at 443 K is very close to 1 As/Ni_t. The amount of C_6 (benzene + cyclohexane) evolved per As fixed (C_6/As_f) is close to 3 for the three samples. Therefore, there is no phenyl group remaining on the sample.

TABLE 4

Triphenylarsine Interaction with Supported Nickel Catalysts at 443 K under 12 bar of H_2 in 50 mL of $AsPh_3$ Solution in *n*-Heptane (14.1 mmol/L)

	NiD10	NiD18	NiD28
Ni_s/Ni_t	0.10	0.18	0.28
As_f/Ni_t	>0.88[a]	1.02	1.03
As_f/Ni_s	7.5	5.6	3.4
C_6/As_f	2.7	3.0	3.0

Note. Amount of triphenylarsine introduced per total nickel atoms ($AsPh_3/Ni_t$) = 1.5. Reaction time: 34 h; quantity of triphenylarsine fixed (As_f), per surface nickel atoms (As_f/Ni_s) or per total nickel atoms (As_f/Ni_t); quantity of C_6 (benzene + cyclohexane) evolved (C_6) per grafted $AsPh_x$ species (C_6/As_f).

[a] The saturation of the sample is not achieved after 34 h of reaction.

3.3. X-ray Diffraction

Figure 7 shows the diffraction patterns of the NiD10 catalyst after reaction with $AsPh_3$ at 303, 373, and 443 K.

After reaction at 303 K (Fig. 7b), the Bragg lines characteristic of Ni particles are present. The integral breadth of the (111) and (200) lines at 44.5° and 51.9° (2θ), respectively, gives an estimate of 7 nm for the Ni crystallite size using the Scherrer equation (19).

The Ni lines disappear totally after reaction at 373 K (Fig. 7c). Small, broad lines are present and can be attributed to a very poorly crystallized Ni_5As_2 phase (orcelite) (20). It is known that solid solutions, the so-called β-

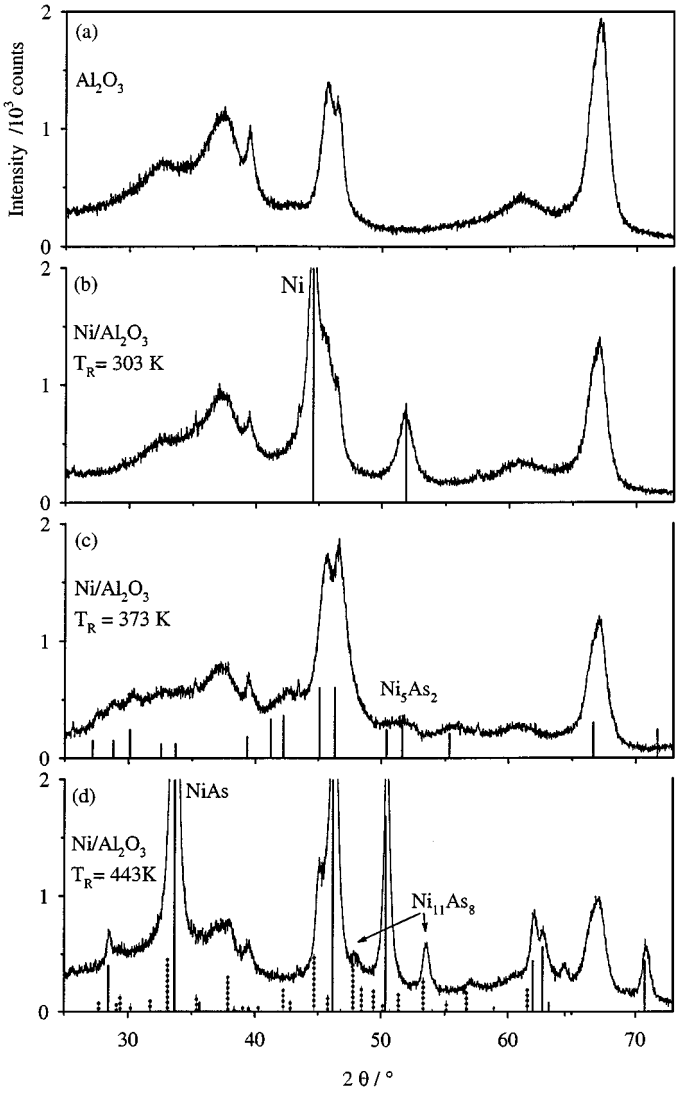

FIG. 7. X-ray diffraction patterns of the alumina carrier (a) and NiD10 catalysts after reaction with $AsPh_3$ at 303 K (b), 373 K (c), and 443 K (d). Vertical bars indicate the position of the Bragg peaks for Ni, Ni_5As_2, NiAs, and $Ni_{11}As_8$ extracted from the powder diffraction file PDF-2 Database (International Center for Diffraction Data).

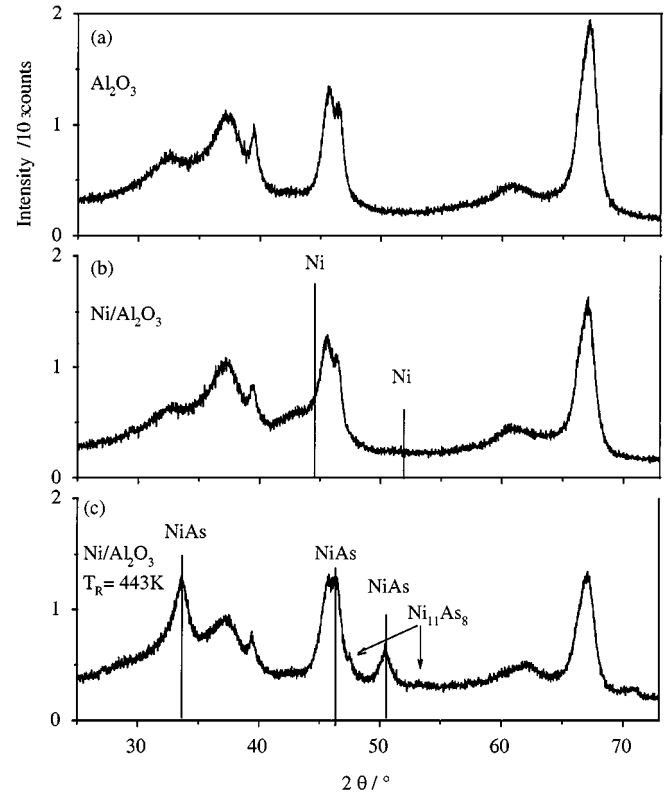

FIG. 8. X-ray diffraction patterns of the alumina carrier (a) and NiD28 catalyst before (b) and after (c) reaction with $AsPh_3$ at 443 K (b).

Ni_5As_2 phase, can exist in the range of composition Ni_5As_2–$Ni_{4.2}As_2$ (21, 22). In these phases, the As/Ni ratio varies between 0.40 and 0.48.

The diffraction pattern of catalyst NiD10 after reaction with $AsPh_3$ at 443 K (Fig. 7d) shows very intense lines at 33.6°, 46.3°, and 50.5° attributed to the NiAs phase (nickeline). The width of the (101) and (110) lines at 33.6° and 50.4° (2θ), respectively, corresponds to a crystallite size of 14 nm. Another phase is present as indicated by weaker lines at 45.1°, 53.5°, and 64.2° corresponding to a $Ni_{11}As_8$ phase (maucherite).

Figure 8 shows the diffraction patterns of the NiD28 catalyst before and after reaction with $AsPh_3$ 443 K. Clearly, the same NiAs (nickeline) and $Ni_{11}As_8$ phases are observed.

3.4. Comparison of the Triphenylarsine and the Tetrabutyltin Interaction with Supported Nickel

At 303 K, under 12 bar of hydrogen, tetra-*n*-butyltin reacts readily with the nickel surface of catalysts NiD10 (Fig. 9), NiD18 (Fig. 10), and NiD28 (Fig. 11).

After about 10 h of reaction, the amount of $SnBu_4$ fixed reached a constant value, which varies from 0.6 to 0.8 Sn_f/Ni_s when the dispersion of the sample increases from 10 to 28%. On the same graphs, the amount of $AsPh_3$ fixed

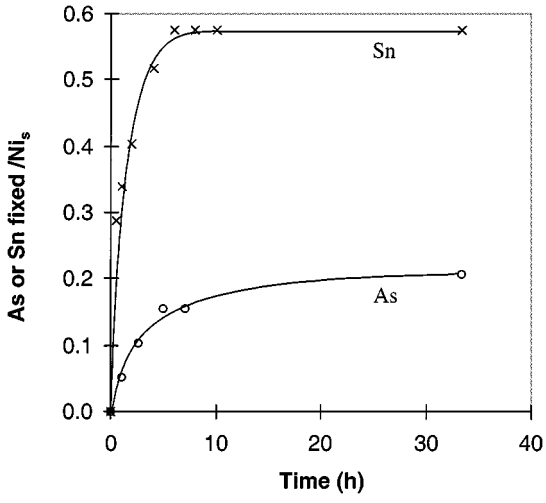

FIG. 9. Grafting of $SnBu_4$ and $AsPh_3$ on Ni/Al_2O_3, NiD10, 50 mL of *n*-heptane, 450 μmol of total nickel, 261 μmol of $AsPh_3$ or $SnBu_4$ ($AsPh_3$ or $SnBu_4/Ni_s = 5.8$), stirring rate = 660 rpm, $T = 303$ K, $P_{H_2} = 12$ bar.

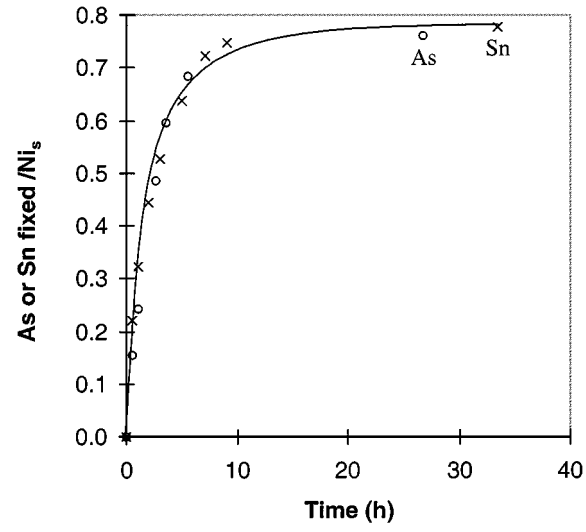

FIG. 11. Grafting of $SnBu_4$ and $AsPh_3$ on Ni/Al_2O_3, NiD28, 50 mL of *n*-heptane, 450 μmol of total nickel, 261 μmol of $AsPh_3$ or $SnBu_4$ ($AsPh_3$ or $SnBu_4/Ni_s = 2.1$), stirring rate = 660 rpm, $T = 303$ K, $P_{H_2} = 12$ bar.

on the nickel surface, in the same conditions of reaction are reported to compare their behavior. It is obvious that the amount of $AsPh_3$ fixed varies with the dispersion of the sample on a much greater scale than $SnBu_4$. For the most dispersed catalyst NiD28 (Fig. 11), the quantities of tetrabutyltin and of triphenylarsine fixed during the reaction process are quite similar. For the two other catalysts (Figs. 9 and 10), the fixed arsenic/surface nickel ratio is lower than the fixed tin/surface nickel ratio and the difference is all the larger since the dispersion of the sample is low.

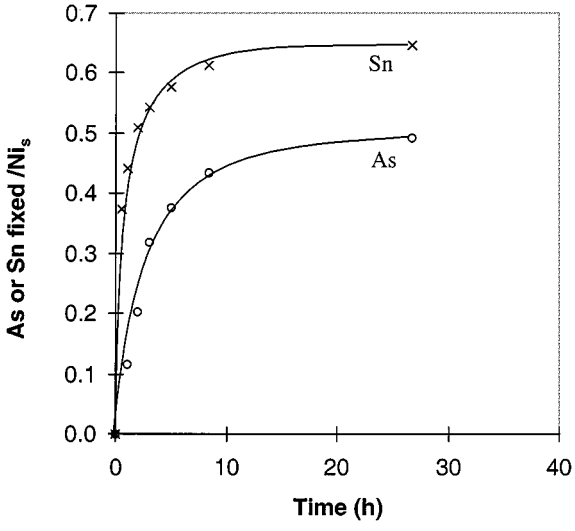

FIG. 10. Grafting of $SnBu_4$ and $AsPh_3$ on Ni/Al_2O_3, NiD18, 50 mL of *n*-heptane, 450 μmol of total nickel, 261 μmol of $AsPh_3$ or $SnBu_4$ ($AsPh_3$ or $SnBu_4/Ni_s = 3.2$), stirring rate = 660 rpm, $T = 303$ K, $P_{H_2} = 12$ bar.

4. DISCUSSION

4.1. T = 303 K: Surface Reaction

At 303 K, the reaction of $AsPh_3$ with Ni is a surface reaction, as demonstrated by the XRD pattern after reaction (Fig. 7b), which shows no change in the Ni particles. There is a discrepancy between the particle size estimated from the dispersion measurement and from the XRD pattern (NiD10). Indeed, a dispersion of 10% corresponds to a particle size of 10–12 nm according to the shape chosen for the model of the particle (18, 19) when XRD gives 7 nm. This is probably due to the fact that the Ni particles present defects (microstrains), which broaden the Bragg lines and therefore decrease the value of the particle size determined by the Scherrer equation.

The As–$(Ph)_3$ bonds hydrogenolysis leads to the formation of the surface species $Ni_s(AsPh_x)_y$. The dispersion of the sample has no effect on the stoichiometry of the grafted AsPh fragments (Table 2) with x (Ph/As_f) close to 1, but has a drastic effect on the coverage of the metallic particle; y (As_f/Ni_s) varies from 0.12 to 0.71. This effect is not observed in the case of $SnBu_4$ reaction with Ni/Al_2O_3 as shown in Figs. 9 to 11 where the coverage of the particles varies slightly from 0.6 to 0.8 Sn_f/Ni_s when the dispersion of the sample increases from 10 to 28%.

The quantity of arsenic fixed by a Ni surface atom increases with the dispersion. This is probably related to the proportion of edge atoms on the surface of the particles. The chemisorption of the fragments –As–Ph can differ according to whether they are grafted onto edge atoms or face atoms of the nickel particles.

TABLE 5

Modelling of Ni/Al_2O_3 Catalysts by Cubooctaedral Particles

Sample	Disp. (%)	m	Diam. (nm)	N_{edge}/N_s	As_f/Ni_s	As_f/N_{edge}
NiD10	10	19	10	0.062	0.20	3.2
NiD18	18	11	5.6	0.109	0.58	5.3
NiD28	28	7	3.6	0.165	0.71	4.3

Note. m, size parameter; N_{edge}, number of surface atoms lying on edges. N_s, number of total surface atoms.

Let us suggest a model for the arsenic adsorption. If we assumed that the shape of nickel particles are cubooctahedral, the total number of atoms (N), the number of surface atoms (N_s), and therefore the dispersion (N_s/N) can be expressed as a function of the value of the size parameter m (the number of atoms lying on an equivalent edge) (13). The values of m fitted to obtain the value of the measured dispersion (Table 1) allow us to calculate the number of surface atoms on the edges of the particle (N_{edge}), the total number of surface atoms on faces (N_s), and the diameter. The results are gathered in Table 5.

The increase of the quantity of fixed arsenic with the proportion of edge atoms (Table 5) means that there are more As–Ph fragments fixed by an edge atom than by a surface atom. Because the range of variation in dispersion is too small, it is impossible to go further numerically. A possible interpretation is tentatively proposed in Fig. 12. The fragments As–Ph are adsorbed flat down on the faces of the nickel particles, both by the arsenic atom and by the phenyl group, occupying several Ni surface atoms (for example, 5 to 10 atoms). On Ni edge atoms, the As–Ph fragment is adsorbed linearly on one edge atom and for very small Ni particles the phenyl groups are not linked to the surface.

4.2. T = 373 K: Formation of the Intermetallic Compound Ni_5As_2

The grafting reaction at 373 K induces a drastic change in the XRD pattern (Fig. 7c). The lines of nickel disappear and a very poorly crystallized phase Ni_5As_2 or/and its solid solution β is detected. This indicates the migration of the naked arsenic atoms inside the nickel particles, which becomes quasi-amorphous. The composition of this phase is consistent with the As_f/Ni_t ratio determined from the reaction (Table 3). Moreover, the Ni_5As_2 phase is rather stable since the composition of this phase is independent of the dispersion when the *pseudo*-plateau is reached, as shown in Fig. 4. Before it, the reaction rate depends on the size of the particles. Indeed, when the dispersion of catalyst increasess, i.e., when the particle size decreases, the reaction rate increases. This can be explained if we assume that the As–Ph bond hydrogenolysis is the limiting step. Thus, the reaction rate is proportional to the number of Ni surface atoms and is faster on the more dispersed catalysts.

4.3. T = 443 K: Formation of the Intermetallic Compound NiAs

At 443 K, independently of the dispersion of the sample, there is formation of a well-defined NiAs alloy (nickeline), characterized by its XRD pattern (Figs. 7d and 8c), as previously observed (9). The composition of this phase is in agreement with the As/Ni_t ratio obtained from the reaction (Table 4). The incorporation of arsenic in the Ni particles produces an increase of the particle size from 7 nm for Ni to 14 nm for NiAs as determined by XRD. Assuming that the lattice volume of Ni and NiAs are respectively 43.76 and 57.29 A^3 and that there are 4 Ni or 2 NiAs per unit cell, for the same number of nickel atoms, the diameter of a NiAs particle must be 2.62 times greater than the diameter of the Ni particle. This value is not so far from the value observed (twice the diameter).

The rate of the two parts of the reaction at 443 K are higher on NiD28 (dispersion = 28%) than on NiD10 (dispersion = 10%), in accordance with the previous observation (10) that the reaction rate at 443 K must be limited by the rate of diffusion of As atoms from the metallic surface to the bulk.

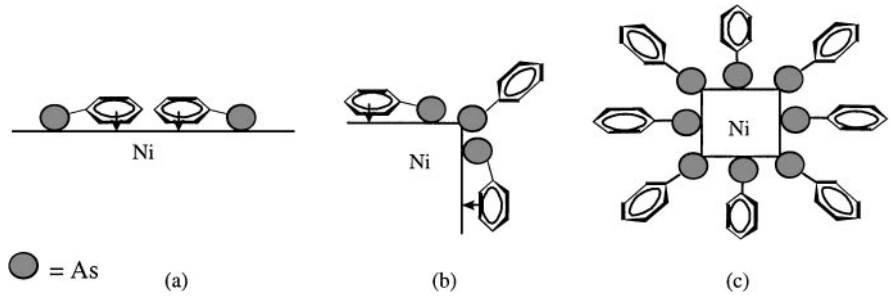

FIG. 12. Proposed models for the adsorption of $AsPh_3$ on Ni/Al_2O_3: (a) on the faces of the Ni particles, (b) on the edges, and (c) on a very small particle.

5. CONCLUSION

The reaction of triphenylarsine with alumina-supported nickel catalysts takes place selectively on the surface of the nickel particles and leads to the successive hydrogenolysis of –As–Ph bonds with benzene and cyclohexane formation.

At 303 K, the reaction stops when the Ni particles are completely covered with grafted –As–Ph fragments. The quantity of fixed arsenic increases with the dispersion of the metal particles. Indeed, more As–Ph fragments (per metallic atom) are grafted onto an edge atom than onto a face atom of the Ni particles.

When the reaction is performed at higher temperature, the As atoms migrate inside the nickel particles easily and form an intermetallic compound. The reaction stops when all the particles are saturated. The Ni_5As_2 phase, very poorly crystallized, is obtained for the triphenylarsine reaction at 373 K. At 443 K the reaction leads to a well-crystallized phase NiAs.

The dispersion of the catalyst has no influence on the nature of the formed intermetallic species. However, the formation rate of these species increases with the dispersion of the catalysts.

This study could thus be extended to other polluting organometallic compounds like PPh_3 or $HgPh_2$.

REFERENCES

1. Ng, C. F., and Chang, Y. J., *Appl. Catal.* **70**, 213 (1991).
2. Ng, C. F., Ye, H., She, L., Chen, H., and Lai, S. Y., *Appl. Catal. A* **171**, 293 (1998).
3. Nielsen, B., and Villadsen, J., *Appl. Catal.* **11**, 123 (1984).
4. Clay, R. D., and Petersen, E. E., *J. Catal.* **32**, 16 (1970).
5. Sarrazin, P., Cameron, C. J., Barthel, Y., and Morrison, M. E., *Oil Gas J.* **9**, 86 (1993).
6. Cameron, C., Cosyns, J., Sarrazin, P., Boitiaux, J. P., and Courty, P., U.S. Patent 5, 601, 701 (1997).
7. Didillon, B., Savary, L., and Uzio, D., French Patent 2, 762, 004 (1997).
8. Didillon, B., Kasztelan, S., and Harle, V., French Patent 2, 762, 214 (1997).
9. Ryndin, Y. A., Candy, J. P., Didillon, B., Savary, L., and Basset, J. M., *C. R. Acad. Sci. Paris Sér. IIc Chim./Chem.* **3**, 423 (2000).
10. Ryndin, Y. A., Candy, J. P., Didillon, B., Savary, L., and Basset, J. M., *J. Catal.* **198**, 103 (2001).
11. Candy, J. P., Didillon, B., Smith, E. L., Shay, T. B., and Basset, J. M., *J. Mol. Catal.* **86**, 179 (1994).
12. Candy, J. P., El Mansour, A., Ferretti, O. A., Mabilon, G., Bournonville, J. P., Basset, J. M., and Martino, G., *J. Catal.* **112**, 201 (1988).
13. Martin, G. A., de Montgolfier, P., and Imelik, B., *Surf. Sci.* **36**, 675 (1973).
14. Stockmeyer, R., Conrad, H. M., Renouprez, A., and Fouilloux, P., *Surf. Sci.* **49**, 549 (1975).
15. Selwood, P. W., "Chemisorption and magnetization." Academic Press, New York, 1976.
16. "Handbook of Chemistry and Physics, 77th Edition, 1996–1997" (D. R. Lide, Ed.), p. 12–115.
17. De Montgolfier, P., Martin, G. A., and Dalmon, J. A., *J. Phys. Chem. Solids* **34**, 801 (1973).
18. Van Hardeveld, R., and Hartog, F., *Surf. Sci.* **15**, 189 (1969).
19. Bergeret, G., and Gallezot, P., *in* "Handbook of Heterogeneous Catalysis" (G. Ertl, H. Knözinger, and J. Weitkamp, Eds.), Vol. 2, pp. 439–464. Wiley-VCH, Weinheim, 1997.
20. Kjekshus, A., and Skaug, K. E., *Acta Chem. Scand.* **27**, 582 (1973).
21. Oen, I., *Bull. Mineral.* **103**, 198 (1980).
22. Heyding, R. D., and Calvert, L. D., *Can. J. Chem.* **35**, 1205 (1957).